Coherence and Rydberg Blockade of Atomic Ensemble Qubits

M. Ebert,* M. Kwon, T. G. Walker, and M. Saffman
Department of Physics, University of Wisconsin, 1150 University Avenue, Madison, Wisconsin 53706, USA
(Received 16 January 2015; revised manuscript received 7 May 2015; published 24 August 2015)

We demonstrate $|W\rangle$ state encoding of multiatom ensemble qubits. Using optically trapped Rb atoms, the T_2 coherence time is 2.6(3) ms for $\bar{N} = 7.6$ atoms and scales approximately inversely with the number of atoms. Strong Rydberg blockade between two ensemble qubits is demonstrated with a fidelity of 0.89(1), and with a fidelity of ~1.0 when postselected on a control ensemble excitation. These results are a significant step towards deterministic entanglement of atomic ensembles.

DOI: 10.1103/PhysRevLett.115.093601 PACS numbers: 42.50.Dv, 03.67.-a, 32.80.Rm, 37.10.-x

Qubits encoded in hyperfine states of neutral atoms are a promising approach for scalable implementation of quantum information processing [1]. While a qubit can be encoded in a pair of ground states of a single atom, it is also possible to encode a qubit, or even multiple qubits, in an N-atom ensemble by using Rydberg blockade to enforce single excitation of one of the qubit states [2,3]. Ensemble qubits have several interesting features in comparison to single-atom qubits. Using an array of traps, it is simpler to prepare many ensemble qubits, with $N \geq 1$ for each ensemble, than it is to prepare an array with exactly one atom in each trap, which remains an outstanding challenge [4–6]. In addition, a $|W\rangle$ state ensemble qubit encoding is maximally robust against the loss of a single atom [7], which can be remedied with error correction protocols [8], while atom loss is a critical error for single-atom qubits. Furthermore, an ensemble encoding facilitates strong coupling between atoms and light, an essential ingredient for quantum networking protocols [9] and atomic control of photonic interactions in Rydberg-blockaded ensembles [10]. As the atom-light coupling strength grows with the number of atoms, recent experiments [10,11] and theory proposals [12] are based on ensembles with $N > 100$. We are focused here on studying the physics of ensembles for computational qubits and, therefore, work with smaller ensembles with up to $N \sim 10$ atoms.

In this Letter we demonstrate and study the coherence and interactions of atomic ensemble qubits. We measure the T_2 coherence time of ensemble qubits, achieving a ratio of coherence time to single-qubit π rotation time of ~2600. We furthermore proceed to demonstrate strong Rydberg blockade between two spatially separated ensemble qubits. With the recent demonstration of entanglement between a Rydberg-excited ensemble and a propagating photon [13], these results establish a path towards both local and remote entanglement of arrays of ensemble qubits, which will enable enhanced quantum repeater architectures [14].

The computational basis states of the ensemble qubits are

$$|\bar{0}\rangle = |0_1, \ldots, 0_N\rangle,$$
$$|\bar{1}\rangle = \frac{1}{\sqrt{N}} \sum_{j=1}^{N} |0_1 0_2, \ldots, 1_j, \ldots, 0_N\rangle, \quad (1)$$

where $|0_j\rangle$ and $|1_j\rangle$ are two ground states of the jth atom in an N-atom sample [15]. The state $|\bar{1}\rangle$, which is a symmetric superposition of one of the N atoms being excited, is commonly referred to as a $|W\rangle$ state.

Gate protocols for ensemble qubits differ from the single-atom qubit case [2,16], as all operations must use blockade to prohibit multiatom excitation. Gate operations are performed via the collective, singly excited Rydberg state

$$|\bar{r}\rangle = \frac{1}{\sqrt{N}} \sum_{j=1}^{N} |0_1 0_2, \ldots, r_j, \ldots, 0_N\rangle,$$

where $|r_j\rangle$ is the Rydberg state of the jth atom. A single-qubit rotation $R(\theta, \phi)$ with area θ and phase ϕ between ensemble states $|\bar{0}\rangle, |\bar{1}\rangle$ is implemented as the three pulse sequence $|\bar{1}\rangle \xrightarrow{\frac{\Omega}{\pi}} |\bar{r}\rangle$, $|\bar{r}\rangle \xleftrightarrow[R(\theta,\phi)]{\Omega_N} |\bar{0}\rangle$, $|\bar{r}\rangle \xrightarrow{\frac{\Omega}{\pi}} |\bar{1}\rangle$. Note that the coupling strength between states $|\bar{1}\rangle, |\bar{r}\rangle$ is the single-atom Rabi frequency Ω, while the coupling between $|\bar{0}\rangle, |\bar{r}\rangle$ is at the collective Rabi frequency $\Omega_N = \sqrt{N}\Omega$. Since Ω_N depends on N, the one-qubit gate pulse lengths depend on the number of atoms. A C_Z gate between control and target ensembles c, t is implemented as the three pulse sequence $|\bar{1}\rangle_c \xrightarrow{\frac{\Omega}{\pi}} |\bar{r}\rangle_c$, $|\bar{1}\rangle_t \xleftrightarrow[2\pi]{\Omega} |\bar{r}\rangle_t$, $|\bar{r}\rangle_c \xrightarrow{\frac{\Omega}{\pi}} |\bar{1}\rangle_c$. The C_Z gate pulses do not depend on the number of atoms. The N dependence of the one-qubit gates can be strongly suppressed using adiabatic pulse sequences so that high-fidelity gate operations are possible with small, but unknown, values of N [17].

The experimental setting is as described in [18]. In brief, we prepare a cold sample of ^{87}Rb atoms in a magneto-optical trap and then load a variable number of atoms into optical dipole traps. The dipole traps shown in Fig. 1 are

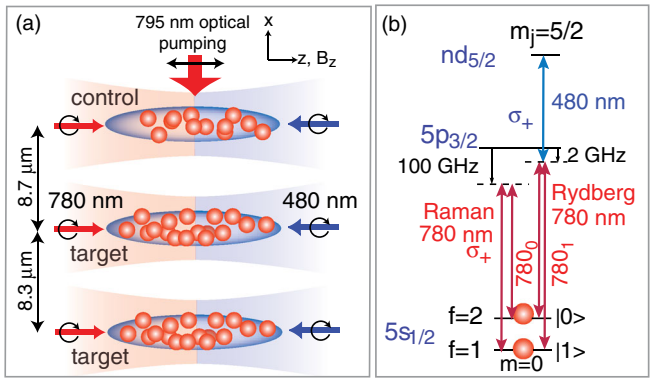

FIG. 1 (color online). Experimental geometry (a) and transitions used for qubit control (b). The Raman light is only used for the preparation of product states, as discussed in connection with Fig. 3.

formed by focusing 1064-nm light to waists ($1/e^2$ intensity radii) of 3.0 μm. The atoms are cooled to a temperature of $\sim$150 μK in 1–1.5-mK deep optical potentials. This gives approximately Gaussian-shaped density distributions with typical standard deviations $\sigma_\perp = 0.7$ μm perpendicular to the long trap axis and $\sigma_z = 7$ μm parallel to the long axis. The estimated density at trap center is $n/N = 5 \times 10^{16}$ m^{-3}. We apply a bias magnetic field along the trap axis of $B_z = 0.24$ mT and optically pump into $|0\rangle \equiv |5s_{1/2}, f=2, m_f=0\rangle$ using π-polarized 795-nm light resonant with $|5s_{1/2}, f=2\rangle \rightarrow |5p_{1/2}, f=2\rangle$ and 780-nm repump light resonant with $|5s_{1/2}, f=1\rangle \rightarrow |5p_{3/2}, f=2\rangle$.

Rydberg excitation coupling $|\bar{0}\rangle, |\bar{r}\rangle$ is performed by off-resonant two-photon transitions via $5p_{3/2}$ [19] using counterpropagating 780_0- and 480-nm light. With σ_+ polarization for both beams, we couple to the Rydberg state $|r\rangle = |nd_{5/2}, m_j = 5/2\rangle$, which is selected with a $B_z = 0.37$ mT bias field. The other qubit ground state is $|1\rangle \equiv |5s_{1/2}, f=1, m_f=0\rangle$. Coupling between $|\bar{1}\rangle, |\bar{r}\rangle$ is performed with 780_1- and 480-nm light, where 780_0 and 780_1 have the same propagation vector and polarization but a frequency difference of 6.8 GHz corresponding to the ^{87}Rb $f=1 \leftrightarrow f=2$ clock frequency. In the experiments reported below we used Rydberg levels $97d_{5/2}$ and $111d_{5/2}$. In both cases strong blockade was observed in individual ensembles, with no evidence for double excitation of the logical $|\bar{1}\rangle$ state [18]. While we do not observe double excitation of $|\bar{1}\rangle$, experiments with two ensembles do show evidence for double excitation of the Rydberg state $|\bar{r}\rangle$, which plays a role in limiting the fidelity with which we can prepare the $|\bar{1}\rangle$ state.

We proceed to demonstrate the coherence of the ensemble states of Eq. (1) using Ramsey interferometry. The amplitude of the Ramsey signal is used to quantify the presence of N-atom entanglement in the ensemble, as has been observed in other recent experiments [20,21]. Details of the analysis showing that $82 \pm 6\%$ of the atoms participate in the entangled $|W\rangle$ state are presented in the Supplemental Material [22]. We load $3 < \bar{N} < 10$ atoms into one of the optical traps. The number of atoms loaded for each measurement follows a Poisson distribution with mean $\bar{N}$. Each measurement starts with optical pumping into $|\bar{0}\rangle$ followed by the pulse sequence

$$|\psi\rangle = R_1(\pi)R_0(\pi/2)R_1(\pi)G(t)R_1(\pi)R_0(\pi/2)|\bar{0}\rangle. \quad (2)$$

Here $R_0(\theta)$ is a pulse of area θ between states $|\bar{0}\rangle, |\bar{r}\rangle$ and $R_1(\theta)$ is a pulse of area θ between states $|\bar{1}\rangle, |\bar{r}\rangle$. The first $R_0(\pi/2)$ pulse creates an equal superposition $(|\bar{0}\rangle + |\bar{r}\rangle)/\sqrt{2}$. This is then mapped to $(|\bar{0}\rangle + |\bar{1}\rangle)/\sqrt{2}$ with a $R_1(\pi)$ pulse; we wait a gap time t described by an operator $G(t)$, map $|\bar{1}\rangle \rightarrow |\bar{r}\rangle$ with a $R_1(\pi)$ pulse, and then perform another $\pi/2$ pulse between $|\bar{0}\rangle, |\bar{r}\rangle$. Finally, any population left in $|\bar{r}\rangle$ is mapped back to $|\bar{1}\rangle$ with another $R_1(\pi)$ pulse. Atoms in state $|0\rangle$ are then pushed out of the trap using unbalanced radiation pressure from a beam resonant with $|5s_{1/2}, f=2\rangle \rightarrow |5p_{3/2}, f=3\rangle$ while the dipole trap light is chopped on and off. For the push-out step a bias field is applied along x, the narrow axis of the dipole traps, and the circularly polarized push-out beam propagates along x. This is followed by a measurement of the number of atoms remaining in the dipole trap, giving the data in Fig. 2. The amplitude of the Ramsey interference at short gap times is limited by the $|W\rangle$ state preparation fidelity of about 50% for the atom number used in the figure. The fidelities of the $R_0(\pi)$ and $R_1(\pi)$ pulses used to prepare $|W\rangle$ are estimated to each be at least 90% on the basis of previous experiments [18] and the strong

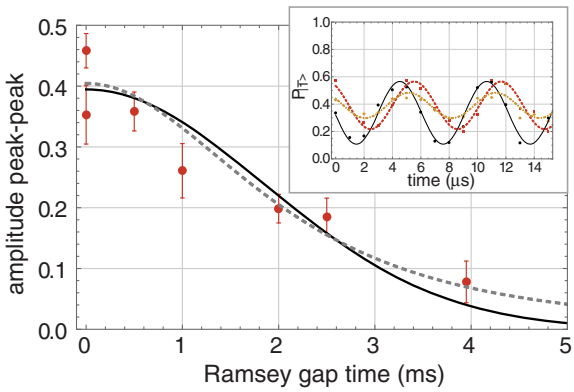

FIG. 2 (color online). Ramsey interference measurement of qubit coherence for $\bar{N} = 7.6$. The peak-peak amplitude of the oscillation as a function of the gap time gives $T_2 = 2.6(3)$ ms. The circles are data points with $\pm\sigma$ error bars and the dashed and solid lines are fits to the functions $v_a(t), v_b(t)$ defined in the text. The gap time is the time t between the $R_1(\pi)$ pulses in Eq. (2). All data have been corrected for $\sim$1.5% probability per atom of the blowaway giving an unwanted transition from $|0\rangle \rightarrow |1\rangle$. The inset shows the Ramsey oscillations for gap times of 0 (solid line), 0.5 ms (dashed line), and 2.5 ms (dashed-dotted line).

interensemble blockade effect we report below. We attribute the limited $|W\rangle$ state preparation fidelity to Rydberg dephasing. Periodic fluorescence measurements of the mean atom number (described in the Supplemental Material to [18]) bound drifts to $6.7 < \bar{N} < 9$, during the 12-h measurement of this data set.

The principal sources of decoherence in this experiment are expected to be magnetic noise, motional dephasing, and atomic collisions [23]. For small atom numbers and low collision rates, we fit the Ramsey signal to the expression [24] $v_b(t, T_2) = v_0/[1 + (e^{2/3} - 1)(t/T_2)^2]^{3/2}$, and in the collision dominated regime we use a Gaussian form $v_a(t) = v_0 e^{-(t/T_2)^2}$, where v_0 is the amplitude at $t = 0$. Both functional forms give the same T_2 time within our experimental error bars of $T_2 = 2.6 \pm 0.3$ ms. The π pulse times were 0.24 μs for $|\bar{0}\rangle \rightarrow |\bar{r}\rangle$, 0.06 μs for the gap between pulses, and 0.68 μs for $|\bar{r}\rangle \rightarrow |\bar{1}\rangle$, giving a coherence-to-$R(\pi)$-gate-time ratio of approximately 2600.

To further clarify the sensitivity to collisional dephasing, Fig. 3 shows the measured T_2 for different $\bar{N}$, including the case of $N = 1$ Fock states which are selected using an additional fluorescence measurement before the Ramsey sequence [18]. We see that $T_2 \sim 1/\bar{N}$, in contrast to the $1/N^2$ scaling observed for Greenberger-Horne-Zeilinger states [25]. The observed $1/\bar{N}$ scaling for $|W\rangle$ states is expected for decoherence dominated by collisions, since the collision rate per atom is proportional to $\bar{N}$. For comparison, the T_2 time was also measured for product states $|\psi\rangle \sim (|0\rangle - i|1\rangle)^{\otimes N}$. These states were prepared using a two-frequency Raman laser coupling $|0\rangle$ and $|1\rangle$ via the $5p_{3/2}$ level [26] as shown in Fig. 1. Comparison of the $|\bar{1}\rangle$ ($|W\rangle$ state) and product-state coherence data suggests that for $N \gtrsim 5$ the coherence time is limited by collisions. For $\bar{N} < 5$ as well as for the $N = 1$ Fock-state data, the product states show a longer coherence time. The coherence of the $|W\rangle$ states is measured by comparison with a phase reference defined by the beat note of the 780_0 and 780_1 Rydberg lasers, which have a measured beat note linewidth of 100-Hz FWHM. This linewidth is consistent with the observed shorter coherence time of the $|W\rangle$ states compared to the product states that are referenced to the Raman laser beat note, which is in turn locked to a stable 6.8-GHz microwave oscillator. We anticipate that compensated optical traps and dynamical decoupling methods, together with an optical lattice to reduce collisional effects, can be used to greatly extend these coherence times [27].

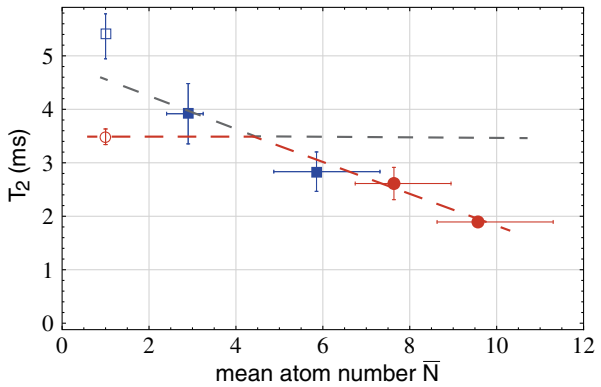

FIG. 3 (color online). Dependence of ensemble coherence time on $\bar{N}$ for $|W\rangle$ states (red circles) and product states (blue squares). The horizontal error bars represent the bounds for atom number measurements interleaved between Ramsey measurements. The open symbols are for preselected $N = 1$ states. The dashed lines are a guide to the eye.

To demonstrate ensemble-ensemble blockade we load atoms into control (c) and target (t) dipole traps, optically pump into $|\bar{0}\rangle_c|\bar{0}\rangle_t$, and apply one of two sequences. Preparation of a superposition of $|\bar{0}\rangle$ and $|\bar{1}\rangle$ in the target qubit is effected by the sequence $U_a|\bar{0}\rangle_c|\bar{0}\rangle_t = R_{1,t}(\pi)R_{0,t}(\theta)|\bar{0}\rangle_c|\bar{0}\rangle_t$. This should ideally leave the qubits in the joint state $|\bar{0}\rangle_c[\cos(\theta/2)|\bar{0}\rangle_t - \sin(\theta/2)|\bar{1}\rangle_t]$ with the probability of preparing $|\bar{1}\rangle_t$ proportional to $\sin^2(\theta/2)$, as is shown in Fig. 4(a). We see the expected time dependence with a peak probability of $P_{|\bar{1}\rangle,t} \sim 0.52$, consistent with our earlier study of Fock-state preparation [18].

Rydberg blockade between two ensembles is observed with the sequence $U_b|\bar{0}\rangle_c|\bar{0}\rangle_t = R_{1,c}(\pi)R_{1,t}(\pi)R_{0,t}(\theta) \times R_{0,c}(\pi)|\bar{0}\rangle_c|\bar{0}\rangle_t$. Here we have used state $|\bar{0}\rangle$ of the control ensemble to block the target transfer with the final $R_{1,c}(\pi)$ pulse ideally leaving the qubits in the joint state $|\bar{1}\rangle_c|\bar{0}\rangle_t$. The data in Fig. 4(a) show a ratio of $P_{|\bar{1}\rangle,t}(U_b)/P_{|\bar{1}\rangle,t}(U_a) = 0.11(1)$, i.e., a blockade fidelity of 0.89. This implies that the success probability of the transition $R_{0,c}(\pi)|\bar{0}\rangle_c \rightarrow |\bar{r}\rangle_c$ is bounded below by the $|\bar{1}\rangle_t$

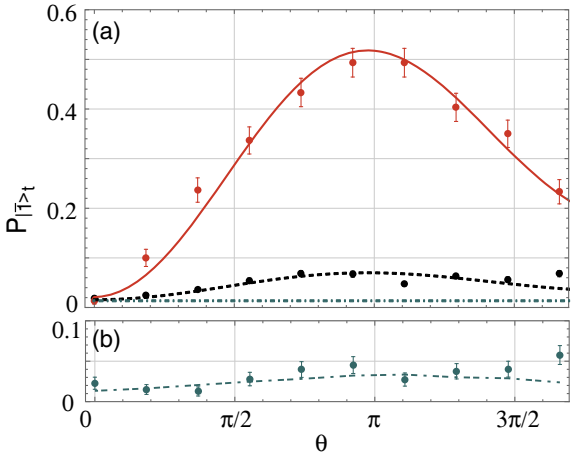

FIG. 4 (color online). Ensemble-to-ensemble blockade for $\bar{N}_c = 9.9$, $\bar{N}_t = 6.2$. (a) Probability of preparing $|\bar{1}\rangle_t$ without blockade (red circles, solid line) and with blockade (black circles, dashed line). The solid line is a fit to a decaying sinusoid function from [18]. The dashed line is the same fit scaled by 11%. (b) Blockade data postselected on the detection of $|\bar{1}\rangle_c$. The dashed-dotted lines in both panels show the expected signal due to state leakage during blowaway in the control and target regions.

population ratio for the two sequences. We infer that at least one atom is excited to the Rydberg state $|r\rangle_c$ with probability $\geq 0.89(1)$.

As a further check on the intersite blockade fidelity, events where the control site ends in state $|\bar{1}\rangle_c$ after the sequence U_b are postselected. The observed postselected target population is shown in Fig. 4(b), along with the expected blowaway leakage rate of the control and target sites, which is measured to be 0.002 per atom. From the data it can be seen that the postselected results are consistent with perfect intersite blockade.

The observed high blockade fidelity exceeds that originally achieved in experiments with single-atom qubits [28,29], and is certainly sufficient to create entanglement between ensemble qubits. What has so far limited a demonstration of deterministic entanglement is the relatively low probability, of up to 62% [18], with which the ensemble state $|\bar{1}\rangle$ can be prepared. In order to gain insight into what is limiting the state-preparation fidelity we looked for signatures of Rydberg-Rydberg interactions concurrently with strong blockade. Ideally the probability of preparing $|\bar{1}\rangle_c$ with sequence U_b should be independent of the pulse area θ applied to the target ensemble. However, a clear dependence on θ can be seen in Fig. 5(a). We believe this effect is due to long-range interactions, where the amplitude for Rydberg atom excitation in the target site is sufficiently blockaded to prevent it from making the transfer to $|\bar{1}\rangle_t$ with any significant probability, yet the target ensemble Rydberg excitation still interacts with the control ensemble strongly enough to disrupt the control ensemble state transfer. A similar situation of partial blockade together with decoherence of multiatom ground-Rydberg Rabi oscillations was reported earlier in [19].

A two-atom Rydberg interaction effect should scale with the Rydberg double excitation probability, i.e., $P_2 \propto \Omega_{\bar{N}}^2/\mathsf{B}^2$, where B is the ensemble mean blockade shift [30]. To check this, we extract the slopes from linear fits to the $P_{|\bar{1}\rangle_c}(\theta)$ data for small θ and compare to the scaling parameter

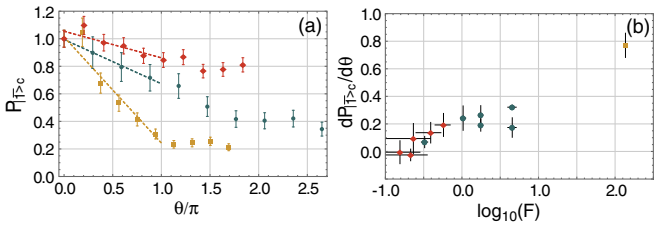

FIG. 5 (color online). Probability of preparing state $|\bar{1}\rangle_c$ as a function of the target ensemble pulse area θ. (a) Probability for several parameter sets: ($111d_{5/2}$, $R = 8.3$ and 8.7 μm) (red diamonds), ($97d_{5/2}$, $R = 8.3$ and 8.7 μm) (green circles), ($97d_{5/2}$, $R = 17$ μm) (yellow squares). The data have been normalized to 1 at $\theta = 0$ for clarity, with typical success probability 40%–60%. (b) Comparison of the slope of the data in panel (a) with the scaling parameter F from Eq. (3). The color markers are the same as in panel (a).

$$F = \Omega_{\bar{N}_t}^2 \left[\frac{(n/n_0)^{12}}{(R/R_0)^6}\right]^{-2} \propto P_{\text{double}}. \quad (3)$$

Here n is the Rydberg principal quantum number and R is the site-site separation. The larger F is for a given set of parameters, the stronger the Rydberg-Rydberg interaction, and, thus, the larger the slope of $dP_{|\bar{1}\rangle_c}(\theta)/d\theta$. Indeed, this is the behavior we observe, as shown in Fig. 5(b), for a range of $\bar{N}$, R, and n.

This interaction effect hints at the possible mechanism responsible for the observed reduction in the probability $P_{|\bar{1}\rangle}$ of preparing the collective qubit state in a single ensemble. The spatial extent of one ensemble is $\sim 2\sigma_z = 14$ μm, giving a length scale in between the lower two data sets in Fig. 5(a). The intraensemble Rydberg interactions are significantly stronger than those between atoms located in different ensembles at the same separation, because the dipole-dipole interaction angular factors favor atom pairs separated along z [30]. These considerations imply that the lack of perfect blockade leading to long-range Rydberg-Rydberg interactions in a single ensemble only partially explains the observed maximum of $P_{|\bar{1}\rangle} = 0.62$ [18]. Another explanation candidate is very strong interactions at short range in a single ensemble that mix levels together and open antiblockade resonance channels [31]. The doubly excited molecular energy structure becomes difficult to calculate with confidence at short range, with many molecular potentials near resonant [32]. For our typical Rydberg state $97d_{5/2}$ this characteristic separation is ~ 5 μm, and for a 6-atom sample with our ensemble spatial distributions an average of 7 atom pairs out of 15 have $R < 5$ μm. We conjecture that the strong short-range interactions give an amplitude for double excitation, resulting in Rydberg-Rydberg interactions that dephase the ground-Rydberg rotations needed for state preparation, and thereby limit the probability of preparing the ensemble $|\bar{1}\rangle$ state. A related reduction of the fidelity of Rydberg-mediated atom-photon coupling in dense ensembles due to Rydberg–ground state interactions has also been observed [11].

In conclusion, we have demonstrated the coherence of ensemble qubit basis states. The coherence time scales approximately inversely with the number of atoms, but is still several ms and 2600 times longer than our characteristic gate time for $N \sim 10$. Additionally we have demonstrated interensemble blockade with a fidelity of 0.89 and ~ 1.0 when postselecting on control ensemble excitation. We identified Rydberg-Rydberg interactions from weak double excitations, either at long or short range, as a possible mechanism limiting the fidelity of ensemble state preparation. Future work towards ensemble entanglement and quantum computation will explore the use of a background optical lattice to better localize the ensembles while limiting uncontrolled short-range interactions.

This work was funded by NSF Grant No. PHY-1104531 and the AFOSR Quantum Memories MURI.

*mebert@wisc.edu

[1] T. D. Ladd, F. Jelezko, R. Laflamme, Y. Nakamura, C. Monroe, and J. L. O'Brien, Nature (London) **464**, 45 (2010).

[2] M. D. Lukin, M. Fleischhauer, R. Cote, L. M. Duan, D. Jaksch, J. I. Cirac, and P. Zoller, Phys. Rev. Lett. **87**, 037901 (2001).

[3] E. Brion, K. Mølmer, and M. Saffman, Phys. Rev. Lett. **99**, 260501 (2007).

[4] W. S. Bakr, J. I. Gillen, A. Peng, S. Fölling, and M. Greiner, Nature (London) **462**, 74 (2009); J. F. Sherson, C. Weitenberg, M. Endres, M. Cheneau, I. Bloch, and S. Kuhr, Nature (London) **467**, 68 (2010).

[5] A. V. Carpentier, Y. H. Fung, P. Sompet, A. J. Hilliard, T. G. Walker, and M. F. Andersen, Laser Phys. Lett. **10**, 125501 (2013).

[6] M. J. Piotrowicz, M. Lichtman, K. Maller, G. Li, S. Zhang, L. Isenhower, and M. Saffman, Phys. Rev. A **88**, 013420 (2013); F. Nogrette, H. Labuhn, S. Ravets, D. Barredo, L. Béguin, A. Vernier, T. Lahaye, and A. Browaeys, Phys. Rev. X **4**, 021034 (2014).

[7] W. Dür, G. Vidal, and J. I. Cirac, Phys. Rev. A **62**, 062314 (2000).

[8] E. Brion, L. H. Pedersen, M. Saffman, and K. Mølmer, Phys. Rev. Lett. **100**, 110506 (2008).

[9] L. M. Duan, M. D. Lukin, J. I. Cirac, and P. Zoller, Nature (London) **414**, 413 (2001); N. Sangouard, C. Simon, H. de Riedmatten, and N. Gisin, Rev. Mod. Phys. **83**, 33 (2011).

[10] T. Peyronel, O. Firstenberg, Q.-Y. Liang, S. Hofferberth, A. V. Gorshkov, T. Pohl, M. D. Lukin, and V. Vuletić, Nature (London) **488**, 57 (2012); V. Parigi, E. Bimbard, J. Stanojevic, A. J. Hilliard, F. Nogrette, R. Tualle-Brouri, A. Ourjoumtsev, and P. Grangier, Phys. Rev. Lett. **109**, 233602 (2012); D. Maxwell, D. J. Szwer, D. Paredes-Barato, H. Busche, J. D. Pritchard, A. Gauguet, K. J. Weatherill, M. P. A. Jones, and C. S. Adams, Phys. Rev. Lett. **110**, 103001 (2013); H. Gorniaczyk, C. Tresp, J. Schmidt, H. Fedder, and S. Hofferberth, Phys. Rev. Lett. **113**, 053601 (2014); D. Tiarks, S. Baur, K. Schneider, S. Dürr, and G. Rempe, Phys. Rev. Lett. **113**, 053602 (2014).

[11] S. Baur, D. Tiarks, G. Rempe, and S. Dürr, Phys. Rev. Lett. **112**, 073901 (2014).

[12] D. Paredes-Barato and C. S. Adams, Phys. Rev. Lett. **112**, 040501 (2014); B. He, A. V. Sharypov, J. Sheng, C. Simon, and M. Xiao, Phys. Rev. Lett. **112**, 133606 (2014); M. Khazali, K. Heshami, and C. Simon, Phys. Rev. A **91**, 030301 (2015).

[13] L. Li, Y. O. Dudin, and A. Kuzmich, Nature (London) **498**, 466 (2013).

[14] Y. Han, B. He, K. Heshami, C.-Z. Li, and C. Simon, Phys. Rev. A **81**, 052311 (2010); B. Zhao, M. Müller, K. Hammerer, and P. Zoller, Phys. Rev. A **81**, 052329 (2010); E. Brion, F. Carlier, V. M. Akulin, and K. Mølmer, Phys. Rev. A **85**, 042324 (2012).

[15] Equation (1) is an approximation to $|\bar{1}\rangle = \sum_{j=1}^{N}(\Omega_j/\Omega_N)|0_1 0_2, \ldots, 1_j, \ldots, 0_N\rangle$ with Ω_j as the Rabi frequency of the jth atom. For our experiments the Rabi frequency is approximately constant across the ensemble, so $\Omega_N = N^{1/2}\Omega$ and Eq. (1) can be written as $|\bar{1}\rangle = N^{-1/2}\sum_{j=1}^{N}|0_1 0_2, \ldots, 1_j, \ldots, 0_N\rangle$.

[16] D. Jaksch, J. I. Cirac, P. Zoller, S. L. Rolston, R. Côté, and M. D. Lukin, Phys. Rev. Lett. **85**, 2208 (2000).

[17] I. I. Beterov, M. Saffman, E. A. Yakshina, V. P. Zhukov, D. B. Tretyakov, V. M. Entin, I. I. Ryabtsev, C. W. Mansell, C. MacCormick, S. Bergamini, and M. P. Fedoruk, Phys. Rev. A **88**, 010303(R) (2013).

[18] M. Ebert, A. Gill, M. Gibbons, X. Zhang, M. Saffman, and T. G. Walker, Phys. Rev. Lett. **112**, 043602 (2014).

[19] T. A. Johnson, E. Urban, T. Henage, L. Isenhower, D. D. Yavuz, T. G. Walker, and M. Saffman, Phys. Rev. Lett. **100**, 113003 (2008).

[20] F. Haas, J. Volz, R. Gehr, J. Reichel, and J. Esteve, Science **344**, 180 (2014).

[21] J. Zeiher, P. Schauß, S. Hild, T. Macrí, I. Bloch, and C. Gross, arXiv:1503.02452 [Phys. Rev. X (to be published)].

[22] See Supplemental Material at http://link.aps.org/supplemental/10.1103/PhysRevLett.115.093601 for analysis of the $|W\rangle$ state entanglement.

[23] M. Saffman and T. G. Walker, Phys. Rev. A **72**, 022347 (2005).

[24] S. Kuhr, W. Alt, D. Schrader, I. Dotsenko, Y. Miroshnychenko, A. Rauschenbeutel, and D. Meschede, Phys. Rev. A **72**, 023406 (2005).

[25] T. Monz, P. Schindler, J. T. Barreiro, M. Chwalla, D. Nigg, W. A. Coish, M. Harlander, W. Hänsel, M. Hennrich, and R. Blatt, Phys. Rev. Lett. **106**, 130506 (2011).

[26] D. D. Yavuz, P. B. Kulatunga, E. Urban, T. A. Johnson, N. Proite, T. Henage, T. G. Walker, and M. Saffman, Phys. Rev. Lett. **96**, 063001 (2006).

[27] Y. O. Dudin, L. Li, and A. Kuzmich, Phys. Rev. A **87**, 031801 (2013).

[28] A. Gaëtan, Y. Miroshnychenko, T. Wilk, A. Chotia, M. Viteau, D. Comparat, P. Pillet, A. Browaeys, and P. Grangier, Nat. Phys. **5**, 115 (2009).

[29] E. Urban, T. A. Johnson, T. Henage, L. Isenhower, D. D. Yavuz, T. G. Walker, and M. Saffman, Nat. Phys. **5**, 110 (2009).

[30] T. G. Walker and M. Saffman, Phys. Rev. A **77**, 032723 (2008).

[31] T. Amthor, C. Giese, C. S. Hofmann, and M. Weidemüller, Phys. Rev. Lett. **104**, 013001 (2010).

[32] A. Schwettmann, J. Crawford, K. R. Overstreet, and J. P. Shaffer, Phys. Rev. A **74**, 020701(R) (2006); T. Keating, K. Goyal, Y.-Y. Jau, G. W. Biedermann, A. J. Landahl, and I. H. Deutsch, Phys. Rev. A **87**, 052314 (2013).